

Ordering phenomena and transport properties of $\text{Bi}_{1/2}\text{Sr}_{1/2}\text{MnO}_3$ single crystals

J. Hejtmánek, K. Knížek and Z. Jirák

Institute of Physics of ASCR, Cukrovarnická 10, 16253 Prague 6, Czech Republic

M. Hervieu and C. Martin

Laboratoire CRISMAT, UMR 6508, ISMRA, Bd du Maréchal Juin, 14050 Caen, France

M. Nevřiva and P. Beran

Institute of Chemical Technology, Technická 5, 16628 Prague, Czech Republic

Measurements of the electrical and thermal conductivities, thermopower and paramagnetic susceptibility have been performed on single crystal samples of $\text{Bi}_{1/2}\text{Sr}_{1/2}\text{MnO}_3$ and complemented with the X-ray powder diffraction data. A pronounced hysteretic behavior, observed below the cubic-to-orthorhombic transition at $T_{crit} = 535$ K, is related to the onset of long-range charge order at $T_{CO} = 450$ K and its further evolution down to about 330 K. The diffraction data suggest that the charge ordered state is formed by Zener pairs, represented by Mn^{4+} dimers linked by one extra e_g electron, and is possibly stabilized by cooperative Bi,Sr displacements. An extremely low thermal conductivity is observed down to the lowest temperatures, without any recovery at the antiferromagnetic ordering temperature $T_N = 150$ K. Such behavior points to a presence of strong scatterers of phonons. Their possible origin can be linked to "optical-like" oscillations which are associated with fluctuating charges within the Zener pairs.

The interest in perovskite manganites with non-integral mean valence ($\text{Mn}^{3+}/\text{Mn}^{4+}$) is associated mainly with their potential to become ferromagnetically ordered and, at the same time, metallic. The origin of such state may be seen in the so-called double-exchange (DE) mechanism [1] that synergically favors fast migration of manganese e_g electrons and ferromagnetic order due to a strong Hund intra-atomic coupling of the itinerant e_g electrons to the localized t_{2g}^3 electrons at Mn sites. On the other hand, the tendency of DE to order the Mn spins ferromagnetically via delocalization of e_g electrons is opposed by strong electron-lattice interactions which prefer the e_g electron localization and result in orbital ordering (Jahn-Teller effect of Mn^{3+} ions), as well as in the $\text{Mn}^{3+}/\text{Mn}^{4+}$ charge ordering effects for particular values of x [2–6].

The typical and often quoted examples of the charge ordered insulators are perovskite $\text{Ln}_{1/2}\text{Ca}_{1/2}\text{MnO}_3$ ($\text{Ln} = \text{La}$ or rare earths). The nature of their state is still under debate. The generally accepted model is Goodenough's orbital scheme [2] based on a chess-board arrangement of the Mn^{3+} and Mn^{4+} valences (Fig. 1a). An alternative model, recently refined by Daoud-Aladine [7,8], is formed by Zener pairs which are represented by Mn^{4+} dimers linked by one extra e_g electron (Fig. 1b). It should be noted that it is very difficult to distinguish between these two structural models and their spin arrangements by the X-ray or neutron powder diffraction

methods, especially for systems with discommensuration defects. In the single crystal diffractometry, the main obstacle is the multidomain character of the charge ordered phase. Nevertheless, for few compounds the conventional chess-board model was unambiguously confirmed even if the actual extent of the charge disproportionation is still uncertain (see e.g. [4,9]). We focus the present paper to a distinct case of $\text{Bi}_{1/2}\text{Sr}_{1/2}\text{MnO}_3$ which exhibits unusually high ordering temperature and we argue that its ordered state can be described by the alternative model.

Previous work on the $\text{Bi}_{1/2}\text{Sr}_{1/2}\text{MnO}_3$ system reported charge ordering at $T_{CO} = 475$ K and pointed to the possible role of the Bi^{3+} lone electron pair in the transition [10]. The characteristic lattice deformation evolves with decreasing temperature and saturates at about 300 K. The fully established charge order at room temperature allowed an electron microscopy study to be performed at atomic resolution [11]. It was shown that the structure of this manganite consists of double stripes of manganese octahedra, and consequently differs from the conventional model. In a low-temperature study an antiferromagnetic ordering of the CE type was detected below $T_N = 155$ K while a minor part of the sample slightly richer on Mn^{4+} showed an A-type order [12]. In contrast to these studies, performed on samples prepared by a ceramic route, the present experiments were undertaken on single crystals grown from high-temperature solutions [13]. The electrical and thermal conductivities and the thermoelectric power were measured between 20 – 900 K using the four point steady-state methods. The high temperature measurements were performed in air and the results were registered both on warming and cooling. The structural characterization was done on pulverized material using the Bruker D8 X-ray diffractometer with $\text{CuK}\alpha$ radiation.

The chemical composition of the $\text{Bi}_{1/2}\text{Sr}_{1/2}\text{MnO}_3$ crystals was verified by Rietveld refinements of powder diffraction data and confirmed (within the experimental error ± 0.02) by electron microanalysis and atomic absorption spectroscopy. In contrast to common $Pbnm$ orthoperovskites, a simpler tilt pattern of the $Ibmm$ symmetry was determined in the present system. The determination of the charge ordered superstructure was attempted in the orthorhombic cell doubled along the b -axis by using two variants - space group $Pnmm$ (con-

ventional model) and $Pn\bar{m}$ (alternative model). The latter model gave a better fit and more realistic oxygen coordination of the Bi,Sr sites confirming that the ordered state in $\text{Bi}_{1/2}\text{Sr}_{1/2}\text{MnO}_3$ is indeed formed by Zener pairs as depicted in Fig. 1b. The picture further shows that the resulting superstructure is associated with a marked transversal modulation in which the interconnected MnO_6 octahedra and the interpolated Bi,Sr are displaced in an opposite phase. The amplitudes of the structural modulation are actually of about 0.1 Å. These findings are in distinction to the conventional charge ordering in other $\text{Ln}_{1/2}\text{A}_{1/2}\text{MnO}_3$ manganites ($\text{A} = \text{Ca}, \text{Sr}$), in which similar modulations are in phase, corresponding to a homogeneous waving of the perovskite lattice as a whole. The different behavior of $\text{Bi}_{1/2}\text{Sr}_{1/2}\text{MnO}_3$ thus strongly suggests that the interpolated large cations, namely Bi^{3+} , play an active role in the charge ordering and are at the root of the exceptionally high charge-ordering temperature T_{CO} . A more detailed inspection of the structural results reveals two different Bi,Sr sites. One, shown at $y = 0$ in Fig. 1b, is slightly shifted upon the charge ordering towards equatorial oxygens of neighboring MnO_6 octahedra along x . The second one, shown at $y = 0.5$, makes an opposite displacement and approaches thus the apical oxygen. Based on the refined Bi,Sr coordinates and Debye-Waller factors it is possible to conclude that the shortest local Bi-O distances are about 2.4 Å. Therefore, there remains an open question of the stereoactivity of the Bi^{3+} lone electron pair which is generally characterized with 2–5 very short Bi-O bonds of 2.2 Å only.

The resistivity data (Fig. 2) show that $\text{Bi}_{1/2}\text{Sr}_{1/2}\text{MnO}_3$ is essentially insulating at low temperatures while at high temperatures well above T_{CO} the electrical resistivity decreases below 10 mΩcm. It is worth mentioning that the observed resistivity is 10^3 lower than the values reported earlier on ceramic samples [12]. The metal-insulator transition is observed at $T_{crit} = 535$ K, *i.e.* above the reported charge ordering temperature, concurrently with a change from the high-temperature cubic $Pm\bar{3}m$ to the orthorhombic $Ibmm$ structure (see the dependence of lattice parameters in Fig. 3). The transition is accompanied by a hysteresis both in the resistivity and in the lattice properties. Closer inspection shows that a marked hysteresis develops below 450 K, which can be related (in reference to the previous work [10]) to the onset of the long-range charge order at T_{CO} . The data further indicate that this broad hysteretic region, characteristic for the 1-st order transition, extends down to ~ 330 K.

The character of the charge carrier conduction and the evolution of the phase transitions at $T_{crit} = 535$ K, $T_{CO} = 450$ K and $T_N = 150$ K are further evidenced by means of the thermopower data, shown also in Fig. 2. Here, the M-I transition at T_{crit} is accompanied by a sharp decrease of the temperature independent thermopower ($S \simeq -35 \mu\text{VK}^{-1}$), which characterizes the adiabatic hopping conduction at higher temperatures. The

large negative values of the thermoelectric power below T_{CO} suggest that the number of conducting electrons is significantly decreased upon charge ordering. On further cooling below the Néel temperature T_N , no substantial change of the electrical resistivity is observed. On the other hand, the value of the thermopower undergoes a distinct decrease at T_N before a final thermodynamic turnover towards zero. This behavior indicates an additional charge carrier localization conditioned by the long range antiferromagnetic order. The low temperature evolution of the thermoelectric power between T_N and 330 K likely mirrors the variable range hopping mechanism of the charge carrier transport when the similar behavior was previously observed for $\text{Sm}_{0.5}\text{Ca}_{0.5}\text{MnO}_3$ ceramics [14].

Finally, the temperature dependence of the thermal conductivity is displayed in Fig. 4. In the charge ordered phase, the thermal transport is solely due to phonon contribution and its low absolute value, which does not show any recovery below T_N , points to an extremely short mean free path of the heat-carrying phonons. This becomes obvious namely in comparison with substantially larger thermal conductivity observed in the conventional charge ordered system $\text{Pr}_{0.5}\text{Ca}_{0.5}\text{MnO}_3$ or with even larger phononic conductivity observed in the ferromagnetic single crystal $\text{Pr}_{0.52}\text{Sr}_{0.48}\text{MnO}_3$ (see Fig. 4).

In summary, the complex study of the $\text{Bi}_{1/2}\text{Sr}_{1/2}\text{MnO}_3$ crystals reveals three phase transitions which manifest themselves in structural, transport and magnetic properties. These are: the cubic-to-orthorhombic transition at $T_{crit} = 535$ K, the onset of long-range charge order at $T_{CO} \sim 450$ K and the antiferromagnetic ordering at $T_N = 150$ K. The structural study and the behavior of inverse susceptibility (see caption of Fig. 2.) suggest that the charge ordered state in $\text{Bi}_{1/2}\text{Sr}_{1/2}\text{MnO}_3$ is formed by Zener pairs and the resulting superstructure is associated with a special kind of Bi,Sr displacements acting cooperatively with the e_g electron ordering. The low thermal conductivity in the ordered phase evidences a presence of strong scatterers of phonons, persisting down to the lowest temperatures. Their possible origin can be linked to "optical-like" oscillations which are associated with fluctuating charges within the Zener pairs.

ACKNOWLEDGMENTS

This work was supported by grants A1010202 and A1010004 of Grant Agency of Academy of Sciences of the Czech Republic.

-
- [1] C.Zener, Phys. Rev. 81 (1951) 440, 82 (1951) 403.
 - [2] J.B.Goodenough, Phys. Rev. 100 (1955) 564.

- [3] P.G.Radaelli *et al.*, Phys. Rev. B 55 (1997) 3015.
- [4] Z.Jiráček *et al.*, Phys. Rev. B 61 (2000) 1181.
- [5] P.G.Radaelli *et al.*, Phys. Rev. B 59 (1999) 14440.
- [6] M.Mizoguchi, J. Phys. Soc. Jpn. 70 (2001) 2333.
- [7] A.Daoud-Aladine *et al.*, Phys. Rev. Letts. 89 (2002) 097205.
- [8] A.Daoud-Aladine *et al.*, *to be published in Applied Physics A*.
- [9] F.Damay, *et al.*, J. Magn. Magn. Mater. 190 (1998) 221.
- [10] J.L.Garcia-Munoz *et al.*, Phys. Rev. B 63 (2001) 064415
- [11] M. Hervieu *et al.*, Chem. Mater. 13 (2001) 1356.
- [12] C. Frontera *et al.*, Phys. Rev. B 64 (2001) 054401
- [13] M. Nevřiva *et al.*, *to be published in Solid State Phenomena*.
- [14] J. Hejtmánek *et al.*, Phys. Rev. B 60 (1999) 14057.

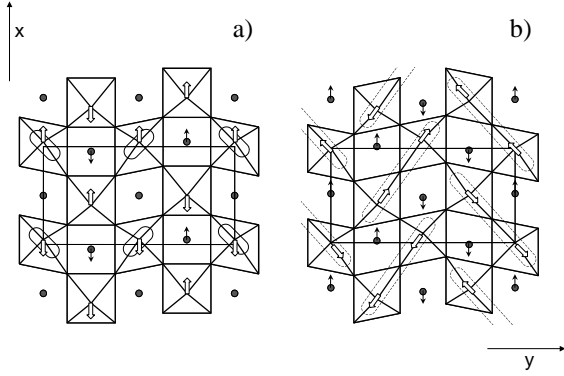


FIG. 1. The (001) perovskite layer in the charge ordered state - (a) conventional model realized in $\text{Pr}_{0.5}\text{Sr}_{0.41}\text{Ca}_{0.09}\text{MnO}_3$ [9] and (b) model of Zener pairs suggested for $\text{Bi}_{1/2}\text{Sr}_{1/2}\text{MnO}_3$. The e_g electron densities in MnO_6 octahedra at plane $z=0$ are schematically shown by the oval shapes; the main displacements of Bi,Sr sites at $z=1/4$ are marked by arrows. The hollow arrows show the spin ordering - (a) antiferromagnetism of the CE type and (b) non-collinear structure expected for the Zener-pair model. (In the plane $z=1/2$ the spins are reversed.) These magnetic arrangements are closely related, since case (b) can be viewed as a superposition of two displaced CE arrangements with spins along x and y , respectively.

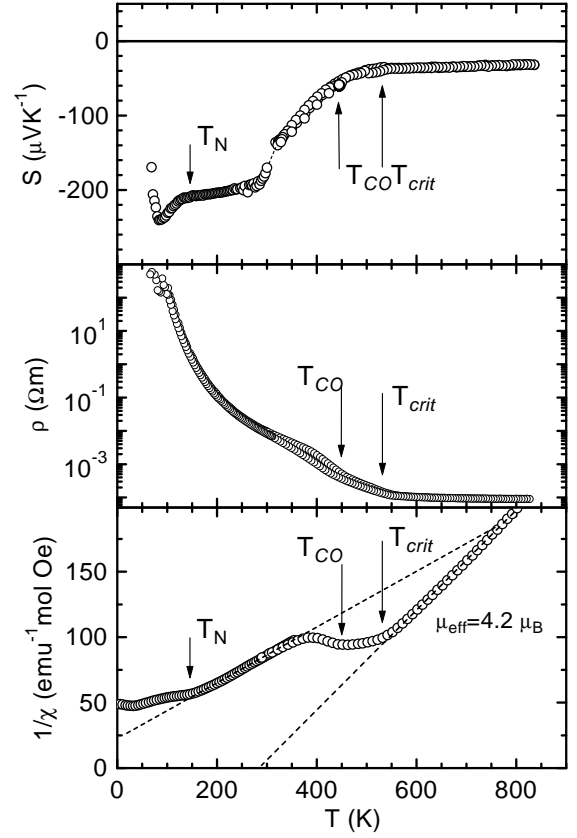


FIG. 2. The temperature dependence of the thermoelectric power (upper panel), electrical resistivity (middle panel) and inverse magnetic susceptibility (lower panel) of the $\text{Bi}_{1/2}\text{Sr}_{1/2}\text{MnO}_3$ crystal. The slope of $1/\chi$ in the charge ordered state for 150 – 300 K closely approaches the value for Zener pairs with total spin $S = 7/2$ ($\mu_{\text{exp}} = 7.83 \mu_B$, $\mu_{\text{theor}} = 7.94 \mu_B$).

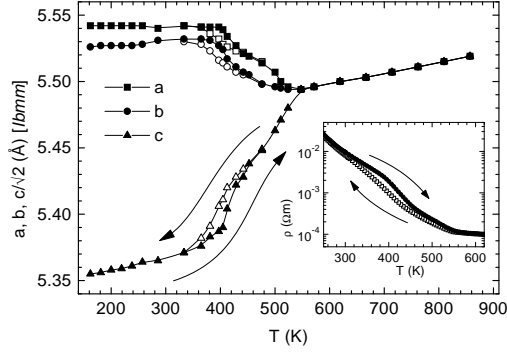


FIG. 3. The temperature dependence of lattice parameters in $\text{Bi}_{1/2}\text{Sr}_{1/2}\text{MnO}_3$. (The inset shows a detail of the resistivity hysteresis upon the charge ordering.)

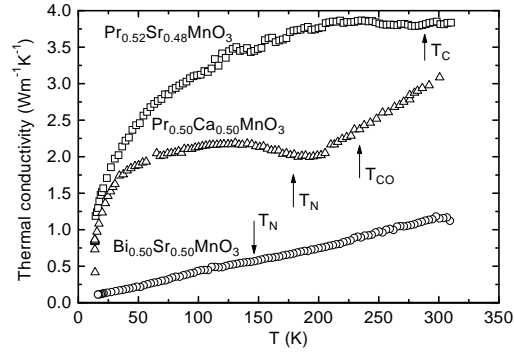


FIG. 4. The temperature dependence of the thermal conductivity in $\text{Bi}_{1/2}\text{Sr}_{1/2}\text{MnO}_3$ compared to the data on charge ordered antiferromagnet $\text{Pr}_{1/2}\text{Ca}_{1/2}\text{MnO}_3$ ($T_{CO} = 240$ K, $T_N = 180$ K) and ferromagnet $\text{Pr}_{0.52}\text{Sr}_{0.48}\text{MnO}_3$ ($T_C = 295$ K; electronic part of thermal conductivity is subtracted).